Appl. Phys. B 63, 593–598 (1996)

Applied Physics B Lasers and Optics

Optical properties and laser performance of neodymium doped scheelites $CaWO_4$ and $NaGd(WO_4)_2$

N. Faure, C. Borel, M. Couchaud, G. Basset, R. Templier, C. Wyon

LETI (CEA-Technologies Avancées), DOPT/SCMDO 17, avenue des Martyrs, 38 054 Grenoble cedex 09, FRANCE
(Fax: (33) 76 88 51 57)

Received: 30 November 1995/Accepted: 21 May 1996

Abstract. Nd-doped $CaWO_4$ (CWO) and $NaGd(WO_4)_2$ (NGWO) single crystals with good optical quality have been grown by the Czochralski technique. The neodymium distribution coefficient in these matrices is about 0.4 for CWO and close to unity for NGWO. Polarized absorption and emission spectra have been recorded at room temperature and used to calculate the absorption and stimulated emission cross-sections.

1 and 2% Nd:CWO and 1% Nd:NGWO laser rods have been tested in a cavity longitudinaly pumped by an 1 W AIGaAs laser diode and compared to Nd:YAG and Nd:YVO_4 rods in the same conditions. The 2% Nd:CWO rod exhibits the best performance with slope efficiencies of 64%, higher than in the case of YAG and equal to the YVO_4 samples. The dependence of the laser output power versus the diode temperature has been measured for all these materials. The laser output of Nd:CWO was found to be nearly as stable as for Nd:YVO_4 and much more stable than in the case of Nd:YAG. A CWO microchip has also been tested for the first time to our knowledge.

PACS: 42.55 R; 42.70; 78

Diode pumped solid state lasers based on neodymium-doped materials (Nd:YAG, Nd:YLF) are now reliable and efficient compact sources. However, typical Nd-doped single crystals exhibit narrow absorption bandwidths in highly ordered structure (like YAG) and precise control of the diode wavelength (hence of the diode junction temperature) is required in order to efficiently pump such crystals. This diode temperature adjustment consumes a lot of energy and thus considerably reduces the wall plug efficiency of the diode pumped solid state laser.

Disordered crystal structures usually present line broadening of both the absorption and emission bands which leads to a decrease in the stimulated emission cross-section of the lanthanide ions and thus in the laser performance. A compromise is then necessary between broad absorption and emission bands like in Nd:$LaMgAl_{11}O_{19}$(LMA) and narrower but more intense ones. Nd:YVO_4, in having good laser performance weakly sensitive to the diode temperature, is a perfect example of such a compromise. Unfortunately, its crystal growth is very difficult and has so far prevented it from being developed industrially.

The search for Nd-doped laser materials that would exhibit the same optical and laser properties as Nd:YVO_4 but which are easier to grow, has lead us to the study of scheelite structure crystals: $CaWO_4$ (CWO) and $NaGd(WO_4)_2$ (NGWO) previously used for flashlamp pumped devices [1–3]. However, because of their low thermal conductivity they were not persued.

1 Crystal structure and growth

$CaWO_4$ (CWO) and $NaGd(WO_4)_2$ (NGWO) crystallyse in the tetragonal system, space group $I4_1/a$. Unlike $KGd(WO_4)_2$ (KGWO) or $KY(WO_4)_2$ (KYWO) [4, 5], they do not exhibit a polymorphic transformation (from the tetragonal $I4_1/a$ space group to the monoclinic C2/c one) below their melting temperature and can thus be grown by the Czochralski technique. Their lattice parameters and other physical properties are shown in Table 1.

Large single crystals (up to 25 mm in diameter and more than 100 mm long) have been grown from the melt using the Czochralski technique. The growth conditions are described in Table 2.

In Nd:CWO charge compensation has been provided by Na^+ doping, whereas no similar substitution is needed of the NGWO matrix, where trivalent neodymium ions substitute also trivalent gadolinium ions. The neodymium distribution coefficient has been measured to be close to unity for NGWO and around 0.4 in CWO. The melt compositions and the corresponding neodymium doping levels between the top and the bottom of the single crystals are then:

- $Ca_{0.98}Na_{0.01}Nd_{0.01}WO_4$ (1% Nd), Nd-doping level between 0.52 and 0.66. 10^{20} at/cm^3,

Table 1. Physical properties of CWO and NGWO

	$CaWO_4$	$NaGd(WO_4)_2$
Lattice parameters (Å)	$a = 5.2429$, $c = 11.373$ (6)	$a = 5.243$, $c = 11.368$ (7)
Density	6.1 (6)	7.2 (7)
Hardness (mohs)	4.5 (8)	
Thermal conductivity ($Wm^{-1}K^{-1}$)	4 (8)	
Melting point (°C)	1580 (8)	1400 (8)
Refractive Index	$n_o = 1.92$, $n_0 = 1.94$ (8)	~1.9

Table 2. Growth conditions of Nd doped CWO and NGWO

	$CaWO_4$	$NaGd(WO_4)_2$
Growth rate (mm/h)	0.9	0.65
Rotation rate (rpm)	10	10
Atmosphere	O_2	O_2
Crucible material	Platinum	Platinum
Seed	Platinum wire	Platinum wire
Nd concentration (at%)	1 and 2	1
Measured distribution coefficient: k_{Nd}	0.4	1

- $Ca_{0.96}Na_{0.02}Nd_{0.02}WO_4$ (2% Nd), Nd-doping level between 1.0 and 1.3. 10^{20} at/cm^3,
- $NaGd_{0.99}Nd_{0.01}(WO_4)_2$ (1% Nd), Nd-doping level around 0.6, 10^{20} at/cm^3.

All crystals are clear, free of cleavage, scattering and color centers and core effect. Some cracks were seen in the top of only one crystal: NGWO.

2 Optical properties

Room-temperature polarized absorption spectra of Nd-doped CWO and NGWO have been recorded on a CARY 5 spectrophotometer. Polarized absorption cross-sections around 800 nm, the zone of interest for the AlGaAs diode pumping, have then been calculated (Fig. 1).

Polarized emission spectra of the same compounds have also been recorded at room temperature using a Ti:sapphire laser tuned to the maximum absorption wavelength λ_a of the laser materials (Table 3).

The absolute emission cross-sections around 1.06 μm have then been calculated (Fig. 2), using (1), which is based on the Fuchtbauer Ladenburg theory:

$$\sigma_e^p = \frac{3\beta}{8\pi c n^2 \tau_{rad}} \frac{I^p(\lambda)}{\sum_p (I^p(\lambda)/\lambda^2)\,d\lambda}, \quad (1)$$

where τ_{rad} is the radiative lifetime of the neodymium $^4F_{3/2}$ state, β is the branching ratio corresponding to the transition $^4F_{3/2} \rightarrow {}^4I_{11/2}$, $I^p(\lambda)$ is the fluorescence intensity in arbitrary units for the π-polarization, n is the refractive index of the matrix, and λ is the average emission wavelength.

β has been taken equal to 0.5, an average value for common neodymium-doped laser materials. Measured fluorescence lifetime (~180 μs) has been used instead of the radiative lifetime. Concentration quenching appears to be relatively weak in these Nd-doped tungstates since the fluorescence lifetimes have been measured, respectively, to 180, 159 and 162 μs in 1% Nd:CWO, 2% Nd:CWO and 1% Nd:NGWO.

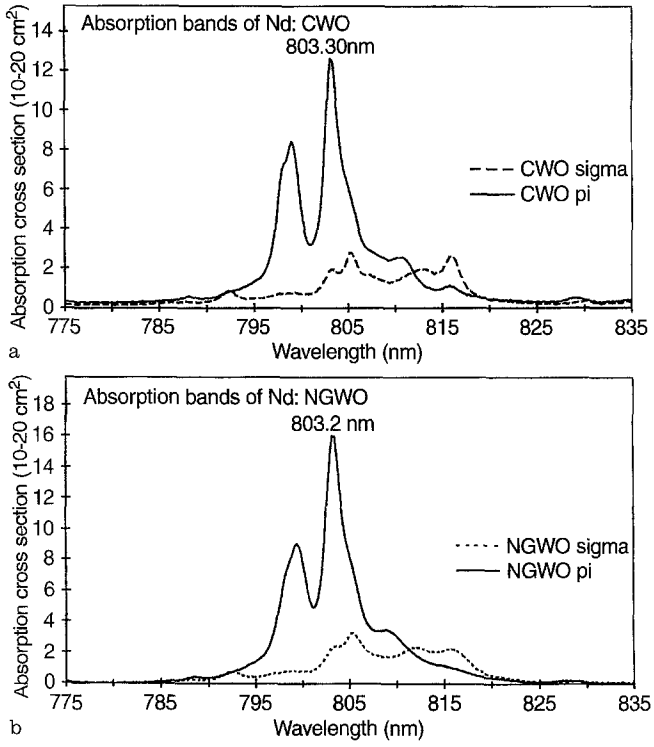

Fig. 1a, b. Absorption bands of Nd:CWO (**a**) and Nd:NGWO (**b**)

Table 3. Optical properties of Nd doped CWO and NGWO

	$CaWO_4$	$NaGd(WO_4)_2$	YAG	YVO_4
λ_a (nm)	803.3	803.2	808.5	808.6
$\Delta\lambda_a$ (nm)	2.6	2.9	1.2	1.4
$\sigma_a(10^{-20}$ cm$^2)$	12.7	16.2	6.3	27
λ_e (nm)	1057.8	1058	1064	1063.5
$\Delta\lambda_e$ (nm)	4.0	12.9	0.8	0.9
$\sigma_e(10^{-19}$ cm$^2)$	1.8	0.94	3.8	6.5

All the data for the absorption and emission bands are collected in Table 3 for the more intense π-polarization. The results for Nd-doped YAG and YVO_4 are also given for comparison.

The absorption bands of Nd-doped tungstates around 800 nm are twice as broad as for Nd:YAG and

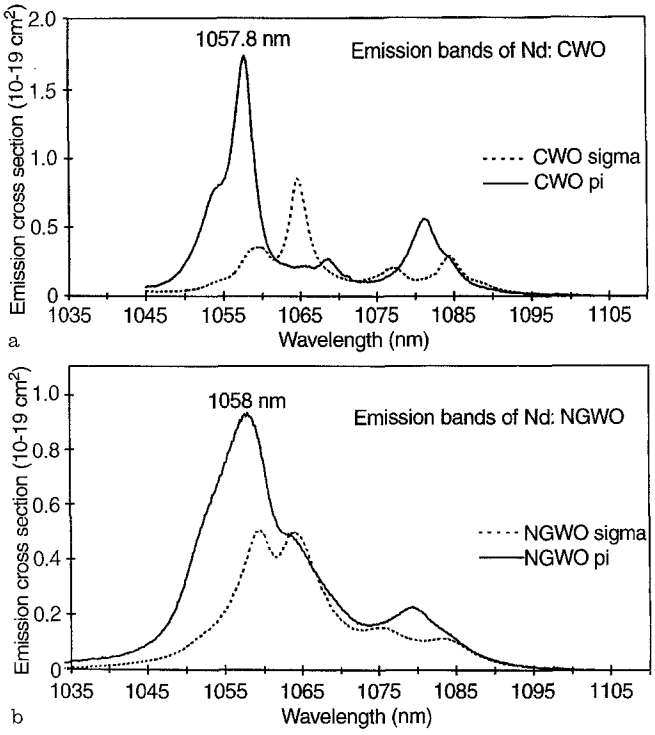

Fig. 2a, b. Emission bands of Nd:CWO (**a**) and Nd:NGWO (**b**)

Nd:YVO_4. The laser performance of the Nd-doped scheelites should therefore be less sensitive to the diode temperature fluctuations.

For microchip applications [9], the length of the active laser material has to be reduced, generally to below 2 mm. To keep relatively high absorbed pump power fractions and thus ensuring high laser performance, the absorption coefficient of the active material must be high. Nd:YVO_4 is again well-suited to this application, whereas in the case of Nd:YAG, short samples exhibit poor laser performance. With their large absorption cross-sections (intermediate between Nd:YAG and Nd:YVO_4), Nd-doped tungstates are thus promising for microchip applications.

3 Laser tests in diode pumping cavity

1 and 2% Nd:CWO, and 1% Nd:NGWO single crystals have been tested in a longitudinally diode pumped cavity. For comparison, Nd-doped YAG and YVO_4 rods have been tested under the same conditions. The pumping device and cavity are described in Fig. 3. A temperature adjusted 1 W SDL 2460 laser diode was used in this experiment. Neutral filters with variable optical densities were used to tune the pump power, thus avoiding the wavelength variations associated with the changes in the laser diode current. The highly divergent beam of the laser diode is collimated, shaped in an anamorphic prism beam expander and focused in the samples. The cavity is plano-concave with an output mirror radius $R_{oc} = 10$ cm and is 5 cm long. The waist of the laser cavity is $\omega_c = 130$ μm.

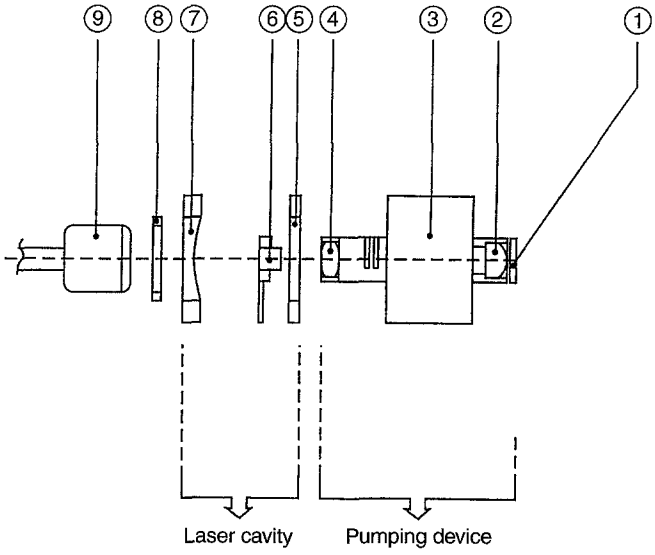

Fig. 3. Experimental device of the diode pumped cavity (1) laser diode, (2) collimating lens, (3) anamorphic prism ($G = X6$), (4) focusing lens, (5) input dichroic plane mirror, (6) laser crystal (diameter: 5 mm, length: 2 or 5 mm), (7) output mirror with Roc = 10 cm, (8) filter, (9) silicon photodiode

The samples were uncoated rods, 5 mm in diameter and 2 or 5 mm long, oriented along the ⟨1 0 0⟩ direction. They were rotated in the cavity to get the $E//c$ (π) configuration, corresponding to the maximum of absorption and emission cross-sections (except for the Nd:YAG isotropic rod).

Using (2) and (3), the optical (ρ_o) and slope (ρ) efficiencies were calculated for each sample, for the incident or absorbed pump power at threshold (P_{inc}^{th} or P_{abs}^{th}) and the incident or absorbed pump power (P_{inc} or P_{abs}) corresponding to the maximum infra-red emitted power (P_{out}), measured in the cavity:

$$\rho_o = \frac{P_{out}}{P_{inc}}, \tag{2}$$

and

$$P_{out} = \rho(P_{abs} - P_{abs}^{th}). \tag{3}$$

Laser performance of all Nd-doped materials tested are presented in Table 4, for the 6.4% output coupler transmission. The corresponding efficiency curves are given in Fig. 4.

Nd:YVO_4 and Nd:YAG, which exhibit the highest emission cross sections also present the smallest threshold values. This is in good agreement with (4), the equation for the absorbed threshold power according to [10]:

$$P_{abs}^{th} = \frac{h\nu_p \pi(T + L)}{4\sigma\tau\eta_p}(\omega_p^2 + \omega_L^2), \tag{4}$$

where $h\nu_p$ is the pump photon energy, η_p is the quantum excitation efficiency, taken equal to 1, ω_s and ω_p are the cavity and pump beam waists, L is the value of the optical losses, and T is the output coupler transmission.

In Nd:CWO, we were expecting lower threshold values (in absorbed power) for the 2 mm long laser rods

Table 4. Laser performance of Nd doped CWO, NGWO, YAG and YVO_4 for the 6.4% output coupler transmission

Crystal	α_a (cm^{-1})	Pinc (mW)	Pout (mW)	Pth inc (mW)	Pth abs (mW)	ρ (%)	ρo (%)
CWO: 1% Nd, 5 mm	4.9	633	217	116	94	55	33
CWO: 1% Nd, 2 mm	4.5	646	104	250	132	48	15
CWO: 2% Nd, 5 mm	6.5	626	286	96	83	64	46
CWO: 2% Nd, 2 mm	9	635	157	163	123	46	25
NGWO: 1% Nd, 2 mm	5.5	594	138	183	109	57	22
YAG: 1.1% Nd, 5 mm	3.4	693	235	77	57	52	34
YVO_4: 1% Nd, 5 mm	11.5	725	390	32	28	64	54

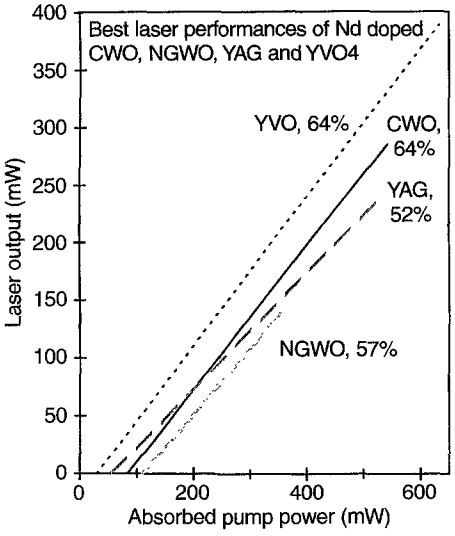

Fig. 4. Laser efficiency curves

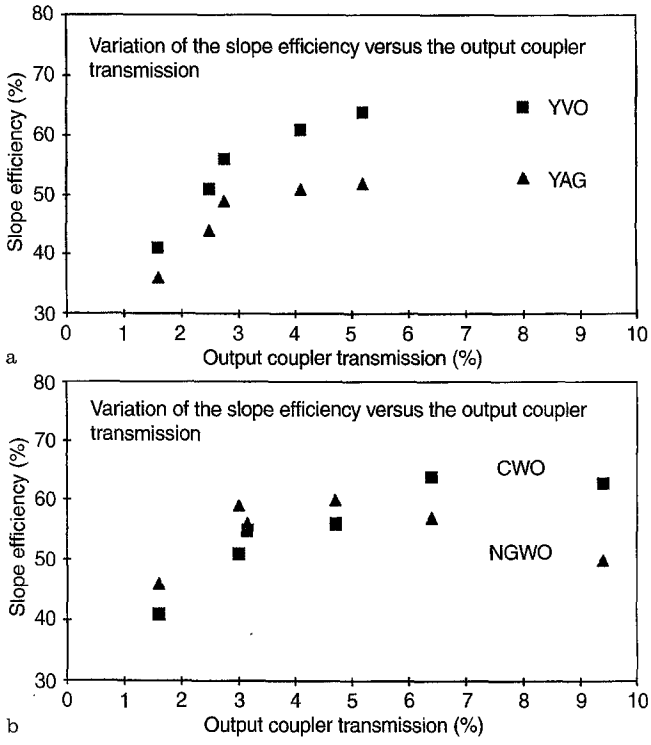

Fig. 5a, b. Evolution of the slope efficiency vs the output coupler transmission: for Nd:YVO and YAG (**a**) and for Nd:CWO and NGWO (**b**)

than for the 5 mm long samples. The experiments, however, showed the opposite behaviour. This result is probably a consequence of the higher optical losses in the 2 mm long rods. Indeed, FIZEAU interferograms have revealed lower double pass wavefront distortions and flatness values for the 2 mm long samples. They are therefore supposed to be more sensitive than the 5 mm long samples to deformation during conditioning operations.

The 5 mm long, 2% Nd:CWO rod shows the best performance, with a relatively low threshold (83 mW absorbed) and a high slope efficiency (64%, identical to YVO_4). The maximum output power measured was nearly 300 mW. The results for the 1% Nd or for the 2 mm long rods are not as good, probably due to weaker Nd-doping level and/or to higher optical losses. A higher Nd-doping level (for example 3% Nd in the melt) may present better results.

The performance of Nd:NGWO are comparable with the 2 mm long Nd:CWO laser rods. Higher doping levels may again show better performance.

The expression for the slope efficiency of a laser (10) is given in (5).

$$\rho = \eta_P \frac{h\nu_L}{h\nu_P} \frac{T}{T+L}, \tag{5}$$

with η_P is the pumping efficiency, taken equal to 1, $h\nu_L/h\nu_P$ is the fraction between the laser and the pumping photons energy, around 0.76 for our materials, T is the output coupler transmission for the laser wavelength, and L is the optical losses in the cavity.

The laser material delivers the maximum slope efficiency thus the maximum output power for the highest output coupler transmissions. Nd-doped YAG, YVO_4 and CWO follow this theory (see Fig. 5): their slope efficiency increases with the output coupler transmission. However, ρ decreases for the highest output coupler transmissions in Nd:NGWO. This can be explained by the inhomogenous broadening of its emission bands (11). Indeed, the sodium and rare earth ions in NGWO occupy the position of the calcium ions in CWO (3). The inhomogenous broadening of the absorption and emission bands is then due to the random filling of the site.

Nd:NGWO thus seems to be less promising than Nd:CWO for high laser output power applications. On the other hand, the neodymium distribution coefficient is close to unity in double sodium gadolinium tungstate whereas it is about 0.4 in CWO. High doping levels, particularly interesting for microchips applications, can

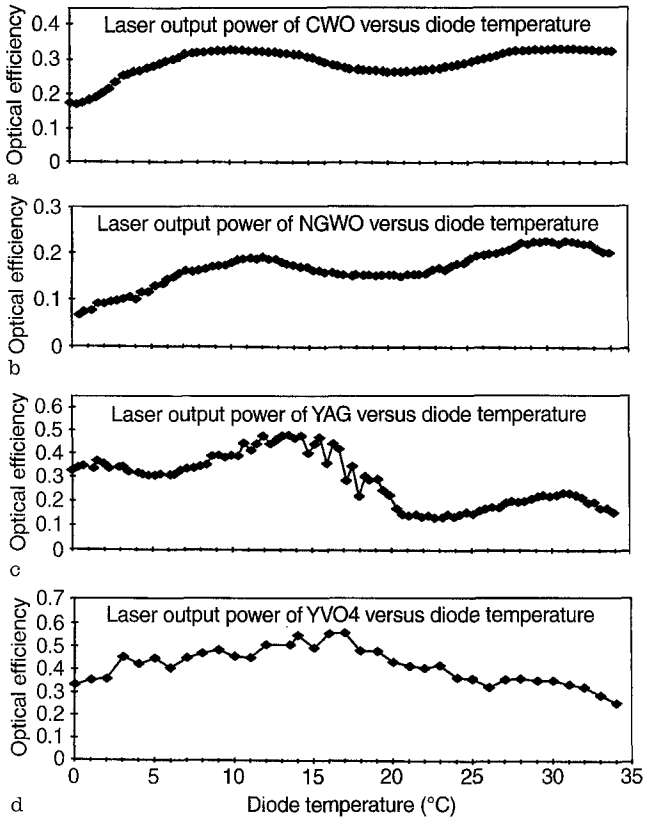

Fig. 6. Evolution of the laser output power vs the diode temperature: for Nd:CWO (**a**), NGWO (**b**), YAG (**c**) and YVO_4 (**d**)

Table 5. Characteristics of the microlasers mirrors

Materials	Nd doping (at %)	Length (mm)	Input mirror		Output mirror	
			T_{810nm}	T_{1064nm}	T_{810nm}	T_{1064nm}
YAG	1.1%	1.1	0.99	0.005	0.35	0.05
YVO_4	1%	2	0.94	0.002	0.85	0.047
CWO	1%	2	0.94	0.002	0.85	0.047

then be more easily reached using NGWO rather than CWO.

The dependence of the laser output power versus the diode temperature has been compared in Fig. 6 for Nd-doped YAG, YVO_4, and the scheelites. As already mentioned in the introduction, the Nd:YAG performance are very sensitive to diode temperature fluctuations. On the contrary, the dependence of the laser output power versus the diode temperature is much weaker for Nd:YVO_4, CWO and NGWO. For Nd:YVO_4 and CWO, the variation in the laser output power is weaker than 20% for a 30° fluctuation on the diode temperature. Nd:CWO is thus of particular interest in diode pumping: it exhibits similar laser performance as Nd:YVO_4 (high slope efficiency and low sensitivity to the diode temperature fluctuations) but is much easier to grow.

A 2 mm long, 1% Nd:CWO microchip has also been tested and compared to Nd-doped YVO_4 and YAG. The dielectric mirrors are deposited directly on the plane and parallel faces of the laser rods (Table 5). The same diode was used to pump these microchips as for the previous laser tests using an external cavity. The microchips performance, in incident power, are shown in Table 6.

Because of its larger absorption cross-section, Nd:CWO performed well: with nearly 180 mW output power (275 mW for YVO_4) and a quite good incident slope efficiency (43% versus 50% for YVO_4). Nevertheless, the threshold value (in incident power) is high for this first test. However, higher Nd-doped crystals would certainly exhibit better performance.

4 Conclusion

The growth and the optical and laser characterisation of Nd-doped scheelites CWO and NGWO have been achieved. Although the samples were not optimized, laser performance were still very good for diode pumped solid state device emitting around 1.06 μm. In particular, the 2% Nd:CWO exhibits the highest output power (more than 280 mW) and slope efficiency (64%), similar to Nd:YAG or Nd:YVO_4 results. Better performance should be obtained with higher doping levels and optimization of the growth and laser parameters. Moreover, the dependence of the output power vs the diode temperature for Nd:CWO is as weak as for Nd:YVO_4 and much weaker than for Nd:YAG. Finally, Nd:CWO is an easier crystal to grow than both the former materials. It is thus, a very good substitute to the vanadates for diode pumping.

The laser performance of Nd:NGWO are not as good. Nevertheless, better results could certainly be obtained for higher doping levels, which can easily be reached since the Nd distribution coefficient is close to unity in this material.

A Nd:CWO microchip laser has been prepared and tested, for the first time to our knowledge. These preliminary results are promising since the 2 mm long, 1% Nd:CWO microchip already delivers 180 mW output power. More heavily doped samples would certainly present higher incident slope efficiency and output power.

In conclusion, the Nd doped scheelites CWO and NGWO are very attractive materials: their optical and laser characteristics are intermediate between those of Nd:YAG and Nd:YVO_4. But their laser performance are

Table 6. Microlasers performance

Materials	Nd doping (at %)	Length (mm)	Threshold (incident power) (mW)	Output power (mW)	Incident slope efficiency (%)
YAG	1.1%	1.1	184	151	23
YVO_4	1%	2	77	275	50
CWO	1%	2	226	179	43

less sensitive to the diode temperature than those of Nd : YAG. Moreover, the tungstates are easier to grow than YVO_4, large size single crystals can thus be obtained. Finally, their high absorption cross-section around 800 nm make them attractive for microchip laser applications.

Acknowledgements. This research was partially supported by Thomson. We wish to thank C. Calvat, Y. Grange and P. Hugot for crystal growth and B. François for conditioning operations.

References

1. L.F. Johnson, G.D. Boyd, K. Nassau, R.R. Soden: Phys. Rev. **126**, 1406–1409 (1962)
2. A.A. Kaminskii, L.S. Kornienko, G.V. Maksimova, P.N. Labenev: Sov. Phys. JETP **22**, 22–25 (1996)
3. G.E. Peterson, P.M. Bridenbaugh: Appl. Phys. Lett. **4**, 173–175 (1964)
4. Chaoyang Tu, Yidong Huang, Zundu Luo, Guang Chen: Crystal Growth, **135**, 636–638 (1994)
5. A.A. Kaminskii, H.R. Verdun, W. Koechner, F.A. Kuznetsov, A.A. Pavlyuk: Sov. J. Quantum Electron. **22**, 10 (1992)
6. JCPDS card 41-1431
7. JCPDS card 25-829
8. J.R. Thomton, W.D. Fountain, G.W. Flint, T.G. Crow: Appl. Opt. **8**, 1087–1102 (1969)
9. J.J. Zayhowski: The Lincoln Laboratory J. **3**, 3, (1990)
10. T.Y. Fan, R.L. Byer: IEEE J. Quantum Electron. **24**, 6 (1988)
11. N. Mermillod, R. Romero, I. Chartier, C. Garapon, R. Moncorgé: IEEE J. Quantum Electronics **28**, 1179–1187 (1992)